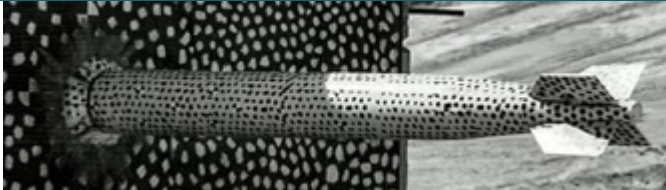
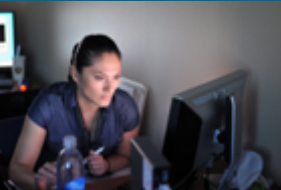




Sandia  
National  
Laboratories

SAND2020-13253C

# Learning continuum-scale models from micro-scale dynamics via Operator Regression

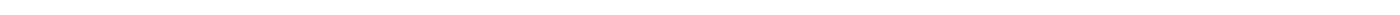


## 14<sup>th</sup> World Congress in Computational Mechanics

Ravi G. Patel, Nathaniel Trask, Mitchell Wood, Eric C. Cyr

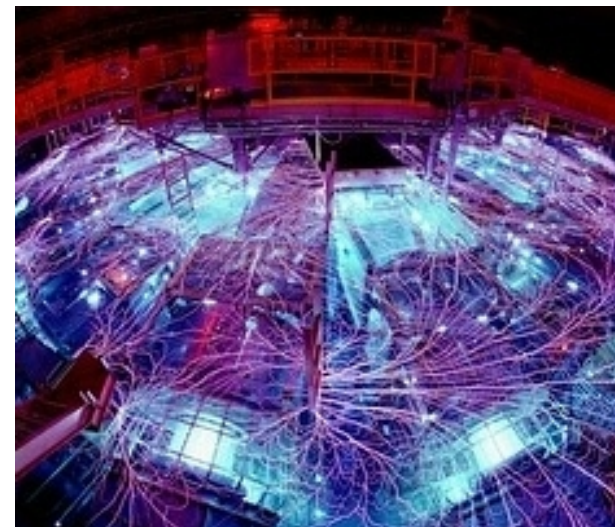
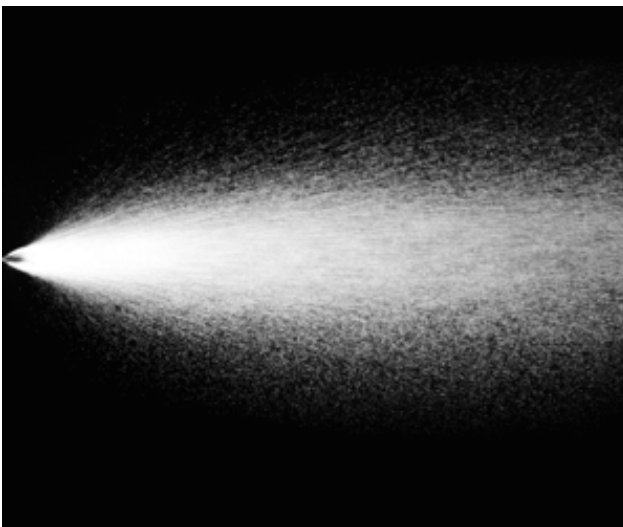
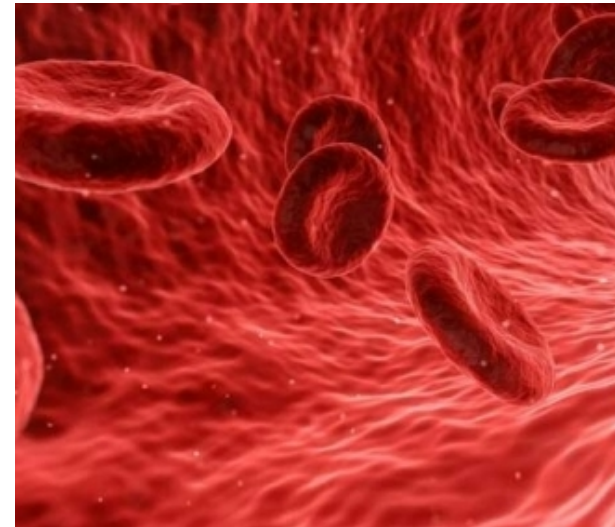
Center for Computing Research

Sandia National Laboratories, Albuquerque, NM, USA



Sandia National Laboratories is a multimission laboratory managed and operated by National Technology & Engineering Solutions of Sandia, LLC, a wholly owned subsidiary of Honeywell International Inc., for the U.S. Department of Energy's National Nuclear Security Administration under contract DE-NA0003525.

## Finding models for multi-scale, multi-physics systems



Given experimental/high fidelity simulation data from a system,

Find a mathematical model that describes the system

Experiments/simulations generate **noisy, biased, sparse** data



### 3 Model power tradeoff



$$\textcolor{red}{F}(u, \dot{u}, x, t) = 0$$

$$\partial_t u + u \cdot \nabla u = -\nabla p + \textcolor{red}{v} \nabla^2 u$$

Black-box ML

?

Parameter  
estimation

Prone to overfitting

Strong assumptions

# Case study: inductive bias in image classification



Translation, scaling, and rotation shouldn't affect an image's class

$$\mathcal{M}[\text{3}] = \mathcal{M}[\text{3}] = \mathcal{M}[\text{3}] = \mathcal{M}[\text{3}]$$

Data augmentation: train with transformed versions of training data

- How thoroughly should transformations be sampled?
- Increased cost of training

Choose model form to have desired invariance/equivariance

- E.g. ConvNets for approximate translational invariance<sup>1</sup>

<sup>1</sup> Lawrence et al. *IEEE Transactions on Neural Networks*, 1997

## Other examples of inductive bias



Rotation invariant model for galaxy classification

- Dieleman et al. *Monthly Notices of the Royal Astronomical Society*, 2015

Warp invariant model

- Wong et al. *DICTA*, 2016

Permutation invariant model

- Meltzer et al. *arXiv:1905.03046*

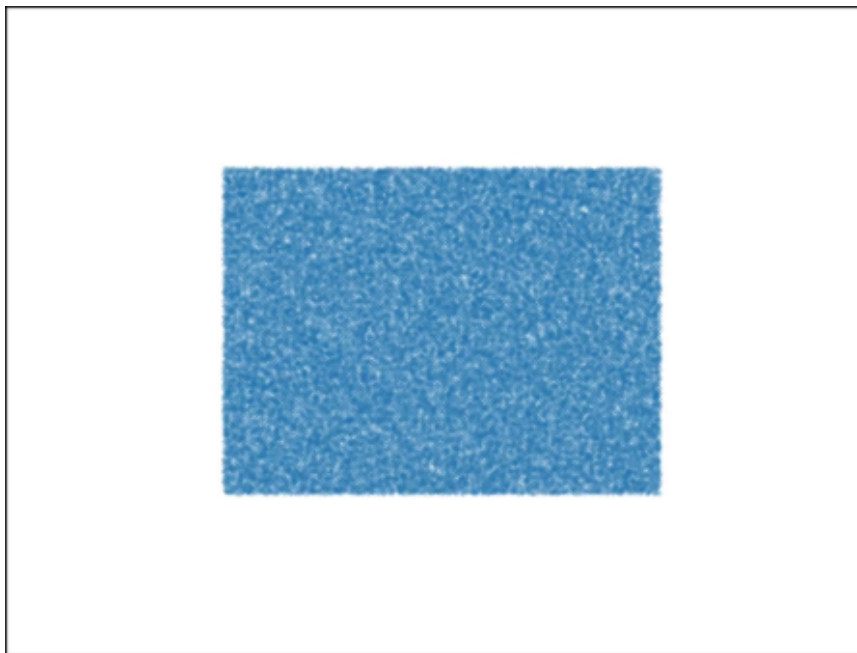
Rotation and translation equivariant model for 3d point cloud data

- Thomas et al. *arXiv:1802.08219*

# Extracting coarse grain models



Find coarse grained dynamics, e.g. evolution of particle density for,



It may be reasonable to assume,

- Conservation
- Translational equivariance
- Rotational equivariance

# Problem statement



Assume system is described by 1<sup>st</sup> order in time, autonomous PDE,

$$\partial_t u = \mathcal{N} u$$

Discretize in time,

$$u^{n+1} = u^n + \Delta t \mathcal{N} u^n = (I + \Delta t \mathcal{N}) u^n$$

Given observations  $\{v^n\}$  , find,

$$\mathcal{N} = \operatorname{argmin}_{\hat{\mathcal{N}}} \sum_n \left\| v^{n+1} - (I + \Delta t \hat{\mathcal{N}}) v^n \right\|$$

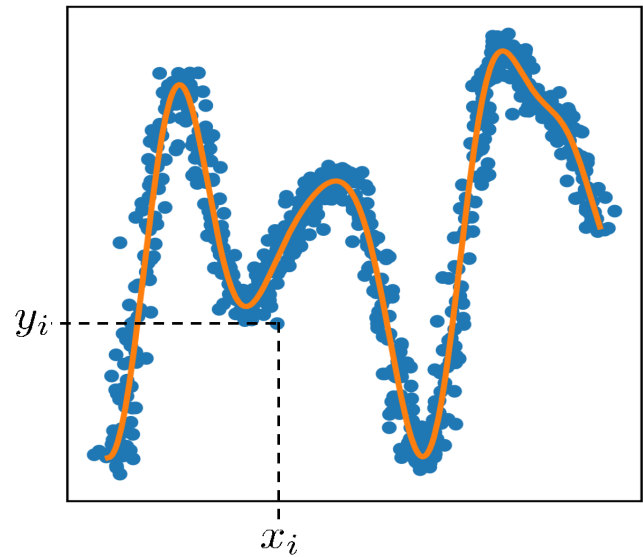
More generally,

$$\mathcal{N} = \operatorname{argmin}_{\hat{\mathcal{N}}} \sum_n \left\| v^{n+p} - (I + \Delta t \hat{\mathcal{N}})^p v^n \right\|$$

# 8 Operator regression

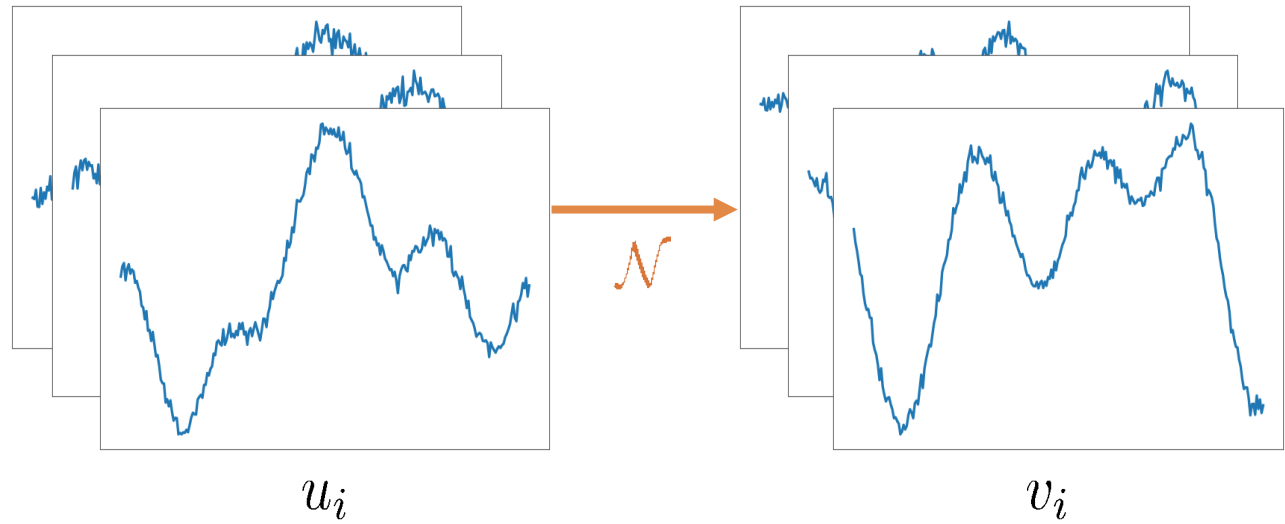


Fitting functions



$$\hat{f} = \operatorname{argmin}_f \sum_i \|y_i - f(x_i)\|$$

Fitting operators



$$\hat{\mathcal{N}} = \operatorname{argmin}_{\mathcal{N}} \sum_i \|v_i - \mathcal{N}[u_i]\|$$

# 9 Modal operator regression for physics (MOR-Physics)



For,

$$u^{n+1} = (I + \Delta t \mathcal{N})u^n$$

Choose,

$$\mathcal{N}u = \mathcal{F}^{-1}g(\kappa; \xi_g)\mathcal{F}h(u; \xi_h)$$

Where  $g$  and  $h$  are neural networks

Optimization problem becomes,

$$\operatorname{argmin}_{\hat{\xi}_g, \hat{\xi}_h} \sum_n \left\| v^{n+p} - (I + \Delta t \hat{\mathcal{N}})^p v^n \right\|$$

Other modal approaches

- Wu and Xiu, *JCP*, 2020
- Li et al. *arXiv:2010.08895*

# MOR-Physics: motivation



For smooth functions in a periodic domain,

Physical space

$$f(x) = \sum_{\kappa} = \tilde{f}_{\kappa} e^{j\kappa x}$$

$$\begin{array}{c} \xrightarrow{\mathcal{F}} \\ \xleftarrow{\mathcal{F}^{-1}} \end{array}$$

Fourier space

$$\begin{aligned} f_{\kappa} &= \int f(x) e^{-j\kappa x} dx \\ (j\kappa)^{\gamma} \tilde{f}_{\kappa} \end{aligned}$$

Parameterization  
contains,

- Laplacian

$$\partial_x^2 u \longrightarrow \mathcal{F}^{-1} [(-\kappa^2) \mathcal{F}[u]]$$

- Advection

$$\partial_x u^2 \longrightarrow \mathcal{F}^{-1} [(j\kappa) \mathcal{F}[u^2]]$$

# MOR-Physics: introducing inductive biases



Translational equivariance:

$$\text{apply } h \text{ point-wise } (h \circ u)(x) = h(u(x))$$

Reflective symmetry: If  $u$  solves the PDE, so does

$$\text{let } h(u) = \text{sign}(u)\tilde{h}(|u|)$$

Isotropy:

$$\text{let } g(\kappa) = \tilde{g}(\|\kappa\|_2^2)$$

Global conservation:

$$\text{let } g(\kappa) = \tilde{g}(\kappa)(1 - \delta_{\kappa,0})$$

# Validation: spatial operator regression in 1D



Given,  $\{u_i, v_i = \partial_x u_i^2\}$  , find,

$$\operatorname{argmin}_{\mathcal{N}} \sum_i \|\mathcal{N}u_i - v_i\|^2$$

$$\text{where } \mathcal{N} = \mathcal{F}^{-1} g(\kappa) \mathcal{F} h(u)$$

assuming translational equivariance

$u_i$  generated from low pass filtered white noise

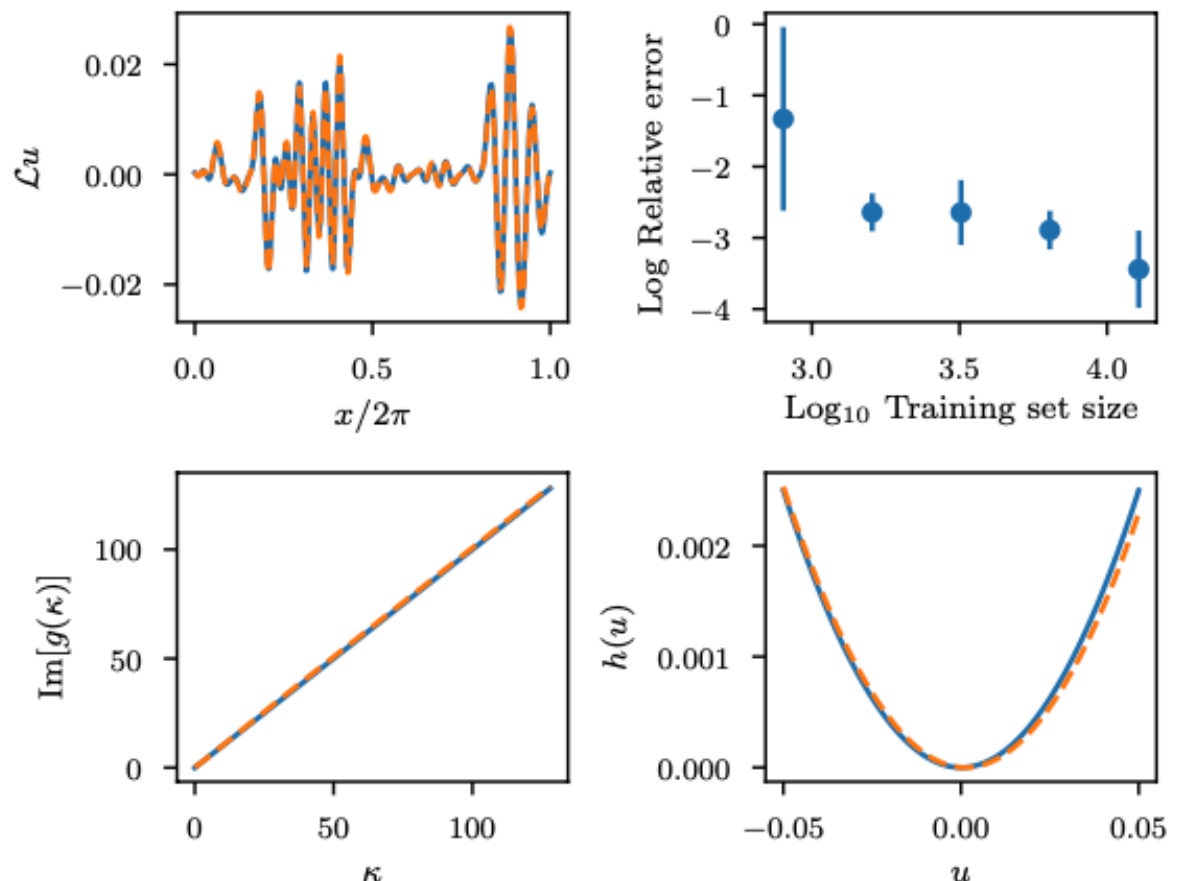


Figure 2: Application of the Burgers operator,  $\partial_x u^2$ , (—) and regressed operator (---) to a function (top left).  $\operatorname{Im}[g(\kappa)]$  (bottom left) and  $h(u)$  (bottom right) for both operators. Relative error,  $\|\mathcal{L}u - \partial_x u^2\| / \|\partial_x u^2\|$  vs. training set size (top right).

# Validation: spatial operator regression in 2D



Given,  $\{u_i, v_i = \Delta u_i\}$  , find,

$$\operatorname{argmin}_{\mathcal{N}} \sum_i \|\mathcal{N}u_i - v_i\|^2$$

where  $\mathcal{N} = \mathcal{F}^{-1}g(\kappa)\mathcal{F}h(u)$

assuming translational equivariance

and compare effect of isotropy

$u_i$   
generated from low pass filtered white noise

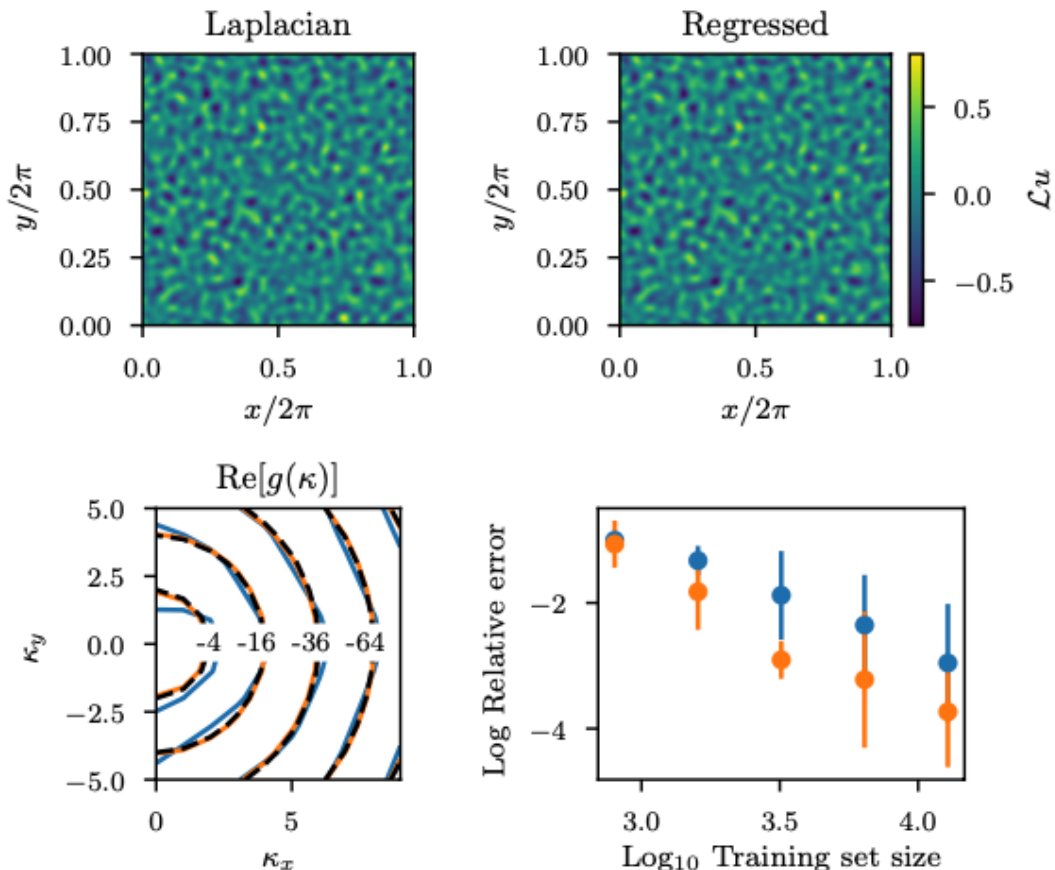
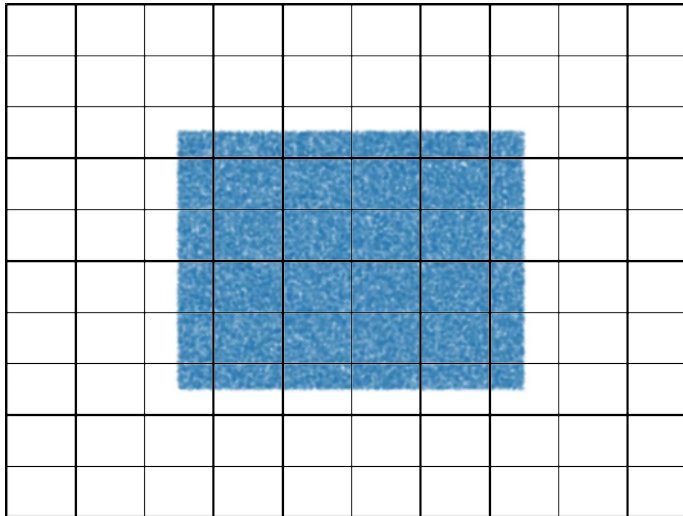
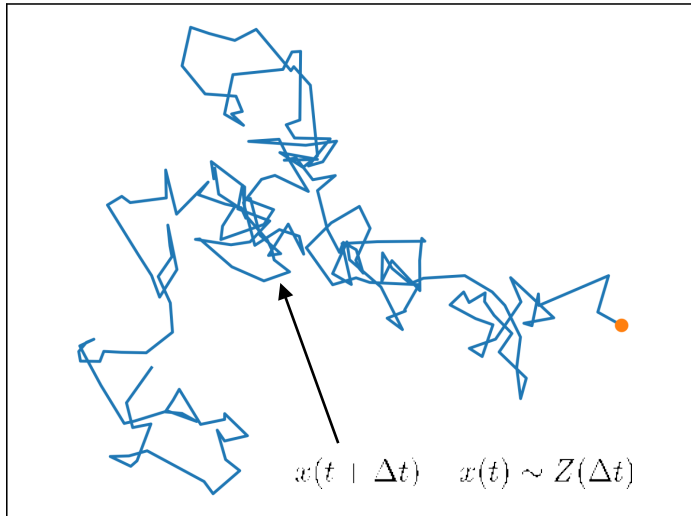


Figure 3: Application of Laplacian to a function,  $\nabla^2 u$ , (top left) and application of the regressed operator with isotropy assumption to the same function,  $\mathcal{L}u$ , (top right). Real part of the symbol of the Laplacian (----), regressed operator without isotropy assumption (—), and regressed operator with isotropy assumption (—) (bottom left). Relative error,  $\|\mathcal{L}u - \nabla^2 u\|/\|\nabla^2 u\|$  vs. training set size (bottom right).

# Coarse graining stochastic differential equations (SDEs)



SDE for particle trajectory → PDE for particle density

1. Compute evolution of binned density from SDE trajectories
2. Fit PDE for evolution of binned density
3. Compare to analytical result

# SDEs: Conservation and reflective symmetry inductive biases improves generalization

Density of Brownian data follows heat equation  $x(t+\Delta t) - x(t) \sim N(0, 2\Delta t) \rightarrow \partial_t u = \Delta u$

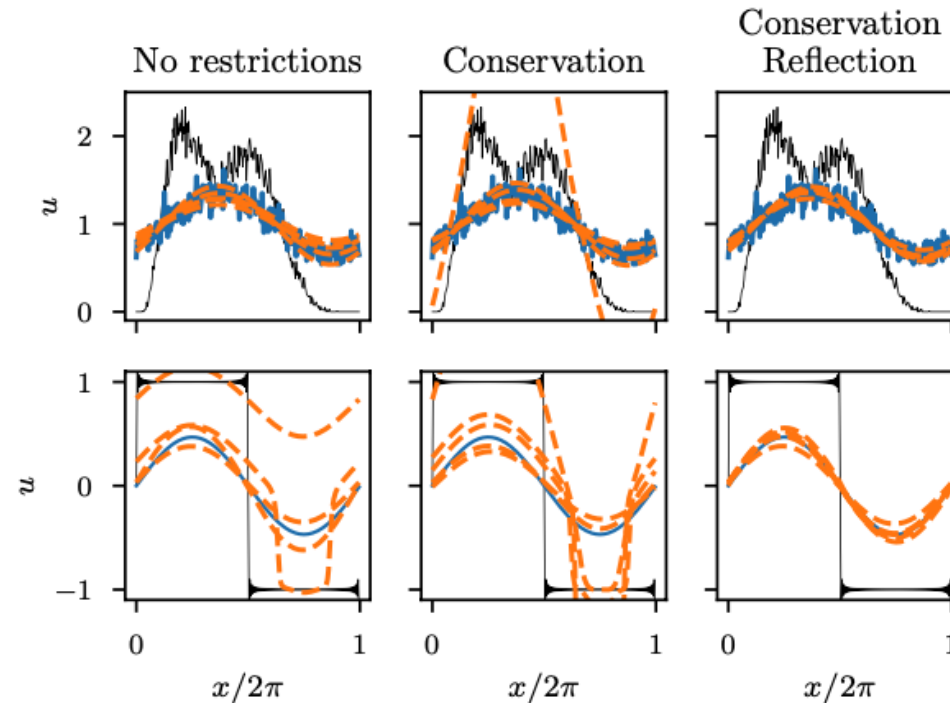


Figure 4: Evolution of the Brownian motion training data (top row) and the heat equation validation example (bottom row) from  $t = 0$  (—) to  $t = 1$  (—) compared to evolution of 5 realizations of the learned equation (—). Each column depicts the final learned solution with different physical assumptions yielding improved training and validation accuracy.

# SDEs: Isotropy inductive bias improves generalization



Density of Levy flight data follows fractional heat equation<sup>1</sup>,

$$x(t + \Delta t) - x(t) \sim L(\alpha, 0, \Delta t^{1/\alpha}, 0) \rightarrow \partial_t u = \Delta^{\alpha/2} u$$

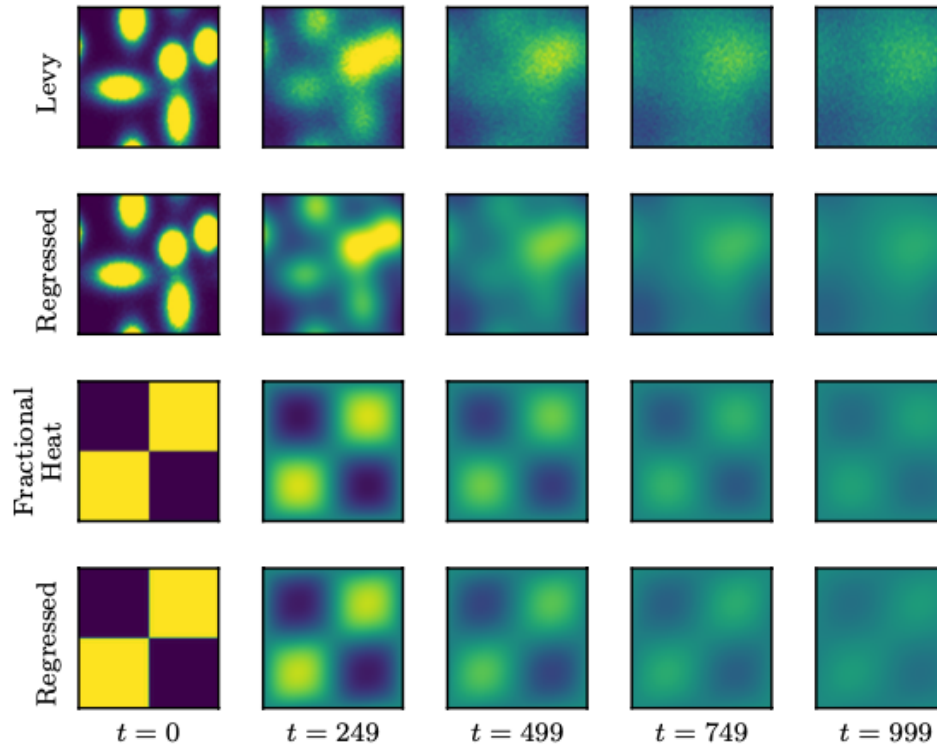


Figure 7: Histograms showing evolution of Levy flight (first row). Evolution of learned operator using histogram of Brownian motion at  $t = 0$  as the initial condition (second row). Evolution of the fractional heat equation with square wave initial condition (third row). Evolution of learned operator on square wave initial condition (fourth row)

# SDEs: Isotropy inductive bias improves generalization



Density of Levy flight data follows fractional heat equation<sup>1</sup>,

$$x(t + \Delta t) - x(t) \sim L(\alpha, 0, \Delta t^{1/\alpha}, 0) \rightarrow \partial_t u = \Delta^{\alpha/2} u$$

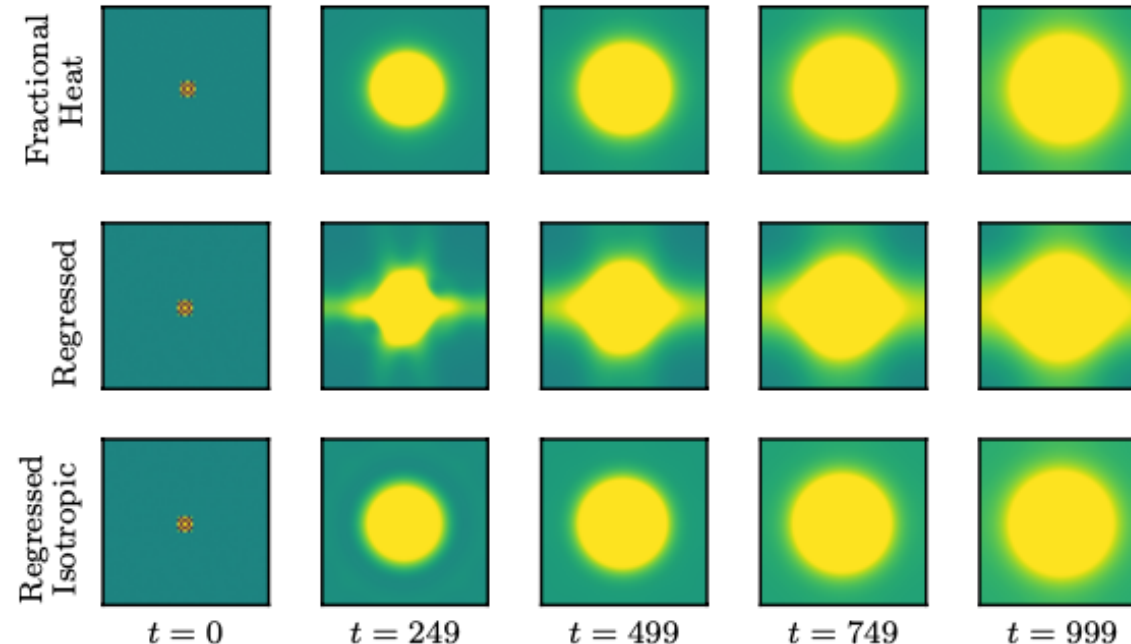
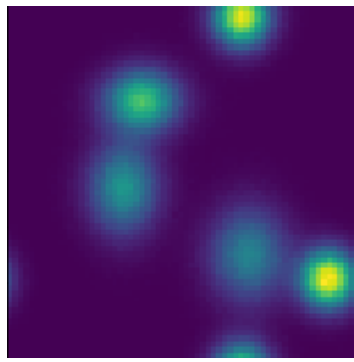


Figure 8: Evolution of the fractional heat equation with Dirac delta initial condition (*first row*). Evolution of the learned equation without isotropy assumption with Dirac delta initial condition (*second row*). Evolution of the learned equation with isotropy assumption with Dirac delta initial condition (*third row*).

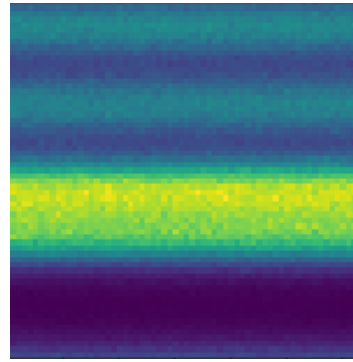
# Isotropy inductive bias counteracts biased data



Vary anisotropy bias in data by setting initial condition,



$$\beta = 0$$



$$\beta = 1$$

Compare effect of isotropy inductive bias for various

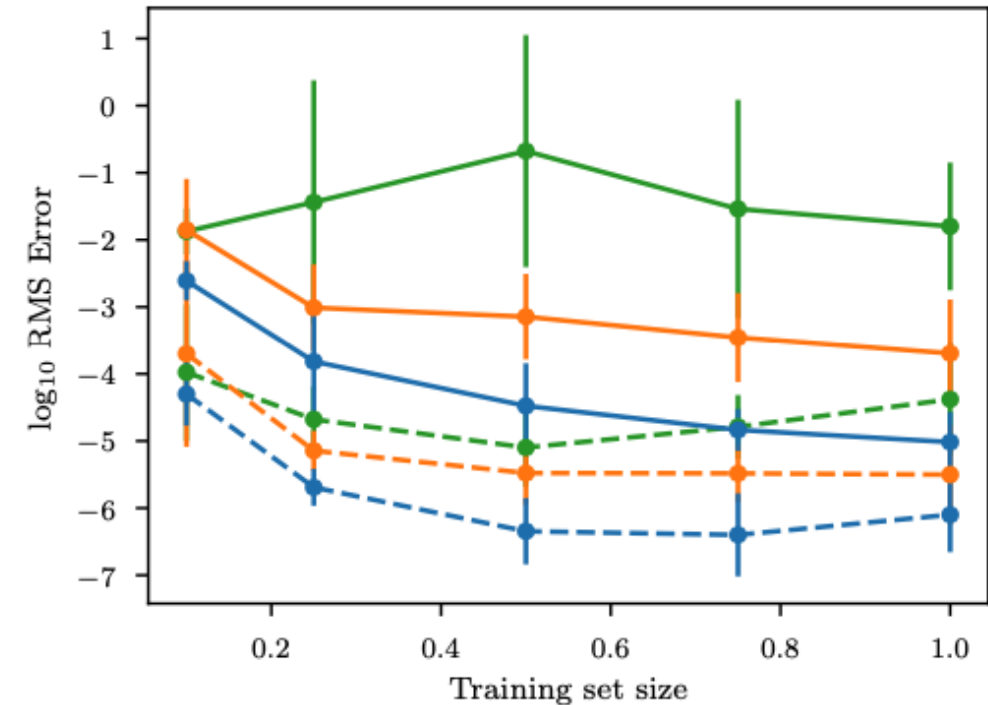
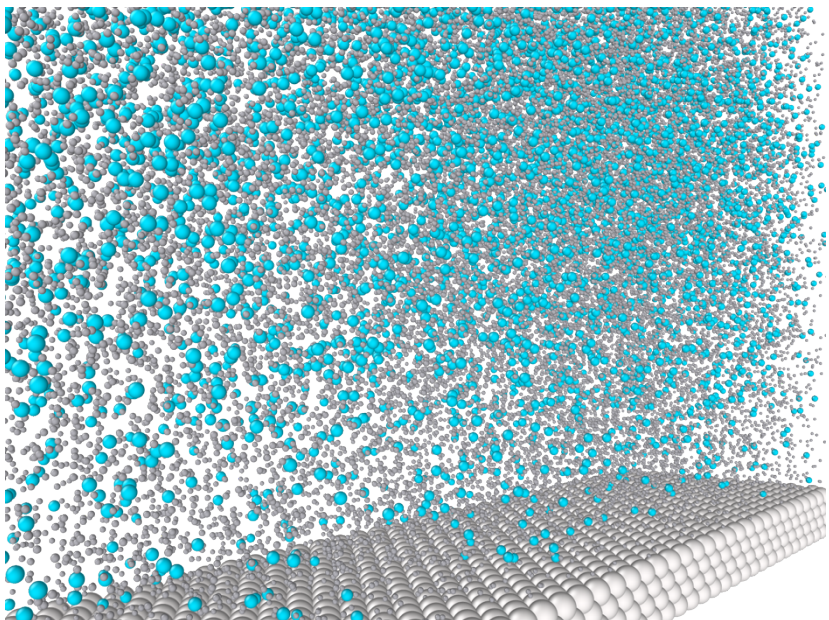
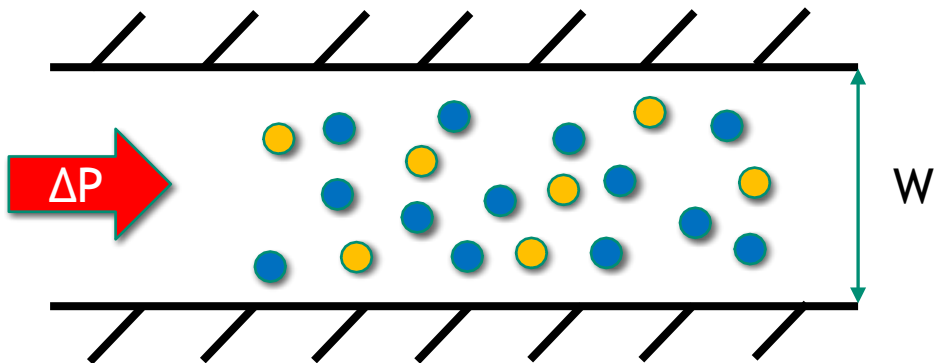


Figure 10: Test error vs. size of training set for anisotropic model trained on data with degree of anisotropy,  $\beta = 0.0$  (solid blue line with circles),  $\beta = 0.1$  (solid orange line with circles), and  $\beta = 1.0$  (solid green line with circles); and for isotropic model trained on data with  $\beta = 0.0$  (dashed blue line with circles),  $\beta = 0.1$  (dashed orange line with circles), and  $\beta = 1.0$  (dashed green line with circles). (statistically isotropic:  $\beta = 0$ ; statistically 1D :  $\beta = 1$ )

# Application: coarse graining colloidal Poiseuille flow



Perform molecular dynamics simulations with varying concentration ( $c$ ), colloid particle size ( $d$ )

- Get time evolution of 1d profiles of

$$\mathbf{u} = (\mathbf{u}_N, \mathbf{u}_D) = ([\rho^L, \rho^S], [p^L, p^S], \dots)$$

Fit continuum model assuming conservation of mass

$$\partial_t u_N^i = \sum_k \mathcal{C}^{-1} g_k^i(\kappa, c, d) \mathcal{C} h_k^i(\mathbf{u}, c, d)$$

$$\partial_t u_D^i = \sum_k \mathcal{S}^{-1} g_k^i(\kappa, c, d) \mathcal{S} h_k^i(\mathbf{u}, c, d)$$

where  $\mathcal{S}$  and  $\mathcal{C}$  are the sine and cosine transform

Find time evolution for new  $c, d$

# Application: coarse graining colloidal Poiseuille flow

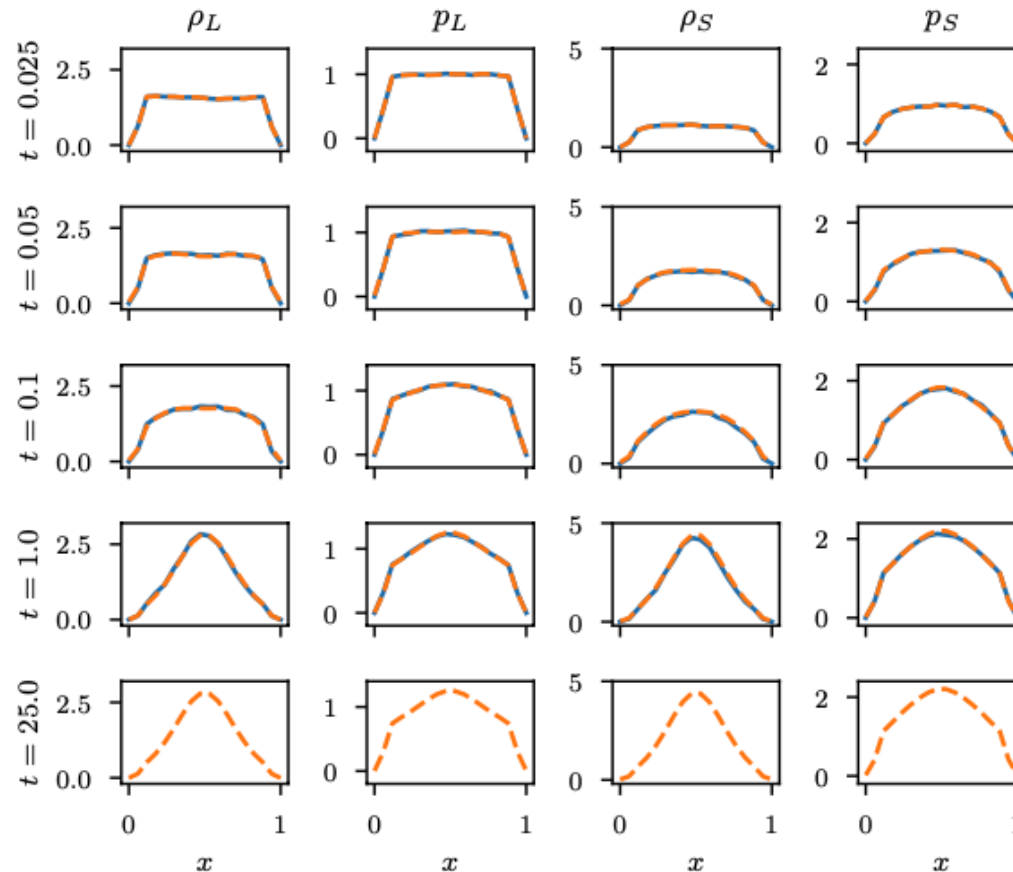


Figure 15: Colloidal system with  $(c, d) = (0.15, 2.5)$ . Evolution of LAMMPS simulation (—) and regressed 4 equation model (---). Small particle density (first column), small particle momentum (second column), large particle density (third column), and large particle momentum (fourth column) is shown for increasing time (rows).

# Future work



Limited to simple geometries and PDEs with smooth solutions

- Alternative basis
  - Generalized moving least squares: Trask et al., *NeurIPS*, 2019

Bayesian version

Noisy data for more general problems

- Error-in-variables models

Applications

Comparisons to other operator regression methods

- Wu and Xiu, *JCP*, 2020
- Li et al. *arXiv:2010.08895*
- Graph Neural operator: Li et al., *NeurIPS*, 2020
- DeepONets: *arXiv:1910.03193*

# Acknowledgements



Eric C. Cyr



Nat Trask

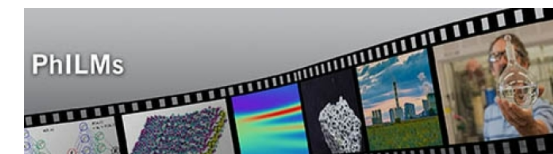


Mitch Wood



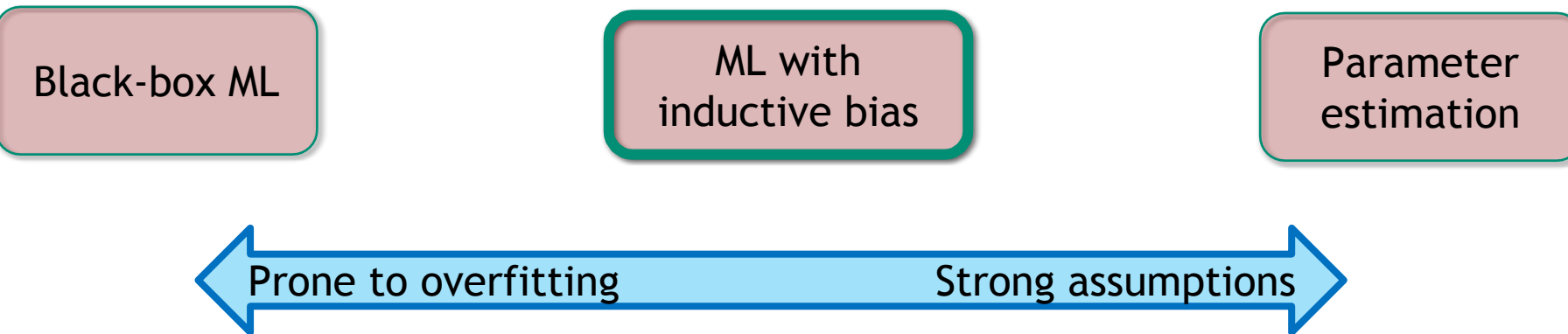
U.S. DEPARTMENT OF  
**ENERGY**

Office of  
Science



[www.pnnl.gov/computing/philm](http://www.pnnl.gov/computing/philm)

# Conclusion



## ML with physics informed inductive biases

- More powerful than parameter estimation
- Better generalization and extrapolation than black-box ML

## Paper and code:

- Patel et al. *CMAME*, 2021 (arXiv:2009.11992)
- <https://github.com/rgp62/MOR-Physics>